Solar RRL
www.solar-rrl.com

Designing Modules to Prevent Reverse Bias Degradation in Perovskite Solar Cells when Partial Shading Occurs

*Eli J. Wolf, Isaac E. Gould, Lyle B. Bliss, Joseph J. Berry, and Michael D. McGehee**

When a solar cell in a panel is shaded, the illuminated cells can place a large reverse bias on the shaded cell to attempt to force current through it. Although the panel can continue to produce power, the reverse bias can cause significant problems for the shaded cell. In the case of perovskite solar modules, Joule heating and irreversible electrochemical reactions will degrade the cell. Some photovoltaic technologies use bypass diodes to solve this problem. To prevent both a perovskite cell and an all-perovskite tandem cell from falling into reverse bias breakdown while shaded, no more than two cells per bypass diode are allowed, which is likely to be prohibitively expensive for many applications. Herein, how many solar cells can be protected by one bypass diode in single-junction and multijunction perovskite modules is explored. It is easier to incorporate bypass diodes into modules with singulated cells than with monolithic panels. It is shown that perovskite–silicon tandems can be protected with fewer bypass diodes than with single-junction perovskite modules. It is suggested that if bypass diodes cannot be feasibly incorporated, then the panels should be deployed in utility-scale power plants.

1. Introduction

Perovskite solar cells have climbed the power conversion efficiency (PCE) ladder quickly over the last decade.[1,2] Now, the small-scale laboratory efficiencies are becoming competitive with silicon and other thin-film technologies, and scale-up techniques and panel design are becoming more important areas of study.[3,4] Although single-junction perovskite photovoltaic cells have reached efficiencies exceeding 25%,[2] tandem architectures have clear pathways to exceeding 30%.[5,6] Perovskite tandem architectures have already achieved the efficiencies of 29.15% for perovskite–silicon tandems, whereas allperovskite tandems have reached 24.8%.[2,7] Commercializing a solar technology from the laboratory to the public market comes with many challenges. One such challenge is the various illumination conditions that are present in the field but not present under a solar simulator. When the amount of light incident on a single cell is reduced, the power output of that cell is temporarily reduced in an approximately linear fashion. In addition, shading a single solar cell operating at maximum power point (MPP) with a simple MPP tracker (MPPT) does not permanently harm the cell. However, fully, or partially shading a single solar cell in a module is different, because the cell is typically connected in series with other power-generating cells. Therefore, when the cell is shaded, it limits the current of all the cells in the module. This not only severely reduces the power output of the entire module during shading, but it can also cause permanent damage to the cell and, therefore, the module. Under certain conditions, the individual cells that are shaded may experience reverse biases greater than their breakdown threshold (**Figure 1**). Typically, this is beneficial to the module power output, as it is more efficient to sacrifice a small amount of voltage in one cell than it is to reduce the current in the entire module. Although the module generates more power when the cell undergoes reverse bias breakdown, this comes at the cost of hot spots localized in the shaded cell. The power dissipated as heat by the shaded solar cell is equal to the breakdown voltage of the cell multiplied by the operating current of the module. Therefore, a shaded cell in reverse bias generates no power and reduces the total power generation of the whole module.

It has been shown that the perovskite solar cells rapidly degrade after briefly passing current in reverse bias. It is likely that this degradation occurs, because there is a high density of holes and essentially no electrons, which creates a situation where iodide can be oxidized to create a high density of iodine vacancies and interstitials.[8–10] There are several consequences of these defects being generated even though, in principle, the vacancies and interstitials can "recombine" after the device is returned to forward bias. First, the interstitials act as nonradiative recombination centers that reduce the current and voltage.

E. J. Wolf
Department of Applied Physics
Stanford University
Stanford, CA 94305, USA

E. J. Wolf, I. E. Gould, L. B. Bliss, Dr. J. J. Berry, Dr. M. D. McGehee
National Renewable Energy Laboratory
Golden, CO 80401, USA
E-mail: michael.mcgehee@colorado.edu

I. E. Gould, Dr. M. D. McGehee
Materials Science and Engineering
University of Colorado
Boulder, CO 80309, USA

L. B. Bliss, Dr. M. D. McGehee
Department of Chemical and Biological Engineering
University of Colorado
Boulder, CO 80309, USA

The ORCID identification number(s) for the author(s) of this article can be found under https://doi.org/10.1002/solr.202100239.

DOI: 10.1002/solr.202100239

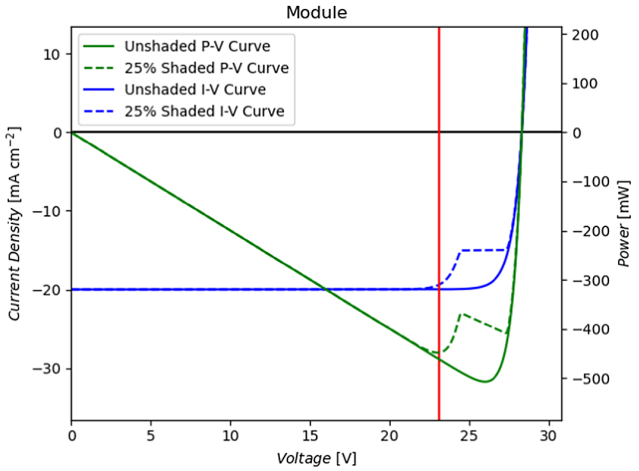

Figure 1. Blue curve: an *I–V* plot of an unshaded(solid line) and partially shaded (dashed line) module. Green curve: a power–voltage curve of an unshaded (solid line) and partially shaded (dashed line) module. Red vertical line: The global MPP of the shaded module. The global MPP of the module forces the shaded cell into reverse bias. The modeled module is made up of 24 cells in series. Even with as little as 25% shading, the global MPP will put the partially shaded cell into reverse bias.

Fortunately, this problem goes away in forward bias when the iodine interstitials are reduced. However, if a cell is briefly shaded and cannot current match the other solar cells for several minutes after the shading event, then the other cells will continue to hold the cell in reverse bias, pinning it in that state until nighttime comes and the cell can recover.[11] Second, Razeraet al. have shown, using scanning transmission electron microscopy coupled to energy-dispersive X-ray spectroscopy, that iodine migrates into the fullerene layer, creating an S-shape in the device current–voltage characteristic.[10] It is believed that the iodine p-type dopes an electron transport layer, causing undesirable interfacial band bending.[10] Third, differing oxidation rates of iodide and bromide into iodine and bromine, respectively, likely cause phase segregation in the perovskite similar to what is observed when bromine-rich perovskites are illuminated.[10] Fourth, the neutral iodine diffuses into the contacts and can potentially leave the perovskite absorber permanently. It is likely that after the iodine leaves the film, it reacts with the electrodes, degrading the device and causing a permanent reduction in PCE.[1,12] In addition, Joule heating can accelerate the natural degradation of the perovskite absorber due to the elevated temperatures associated with localized heating.[13]

As the oxidation of iodide in reverse bias probably cannot be prevented and containing the iodine within the perovskite is challenging, we have explored how modules might be designed to protect perovskite solar cells from being put into reverse bias. For this study, we simulated module *I–V* curves using Kirchhoff's laws to combine cells and bypass diodes in various series and parallel topologies. We develop a model to examine partial shading effects in a module made of cells in series. Our findings provide design rules for both perovskite single-junction and tandem modules whether in a singulated or monolithically integrated implementation. These design rules mitigate potential damage induced by partial shading in the module when individual cells are placed into reverse bias or limit the module current. For an in-depth look at specific details on module design, please refer to the manuscript recently published by Werner et al.[3]

2. Current–Voltage Curves of Partially Shaded Modules

To illustrate what happens when only one cell in a module is shaded, we have modeled a panel with 24 cells in series.[14–18] Each modeled perovskite cell has an open circuit voltage (V_{oc}) of 1.18 V, a maximum power voltage of 1.08 V, a reverse bias breakdown voltage (V_{br}) of 2 V, and a short circuit current (J_{sc}) of 20 mA cm^{-2}, similar to the current state-of-the-art wide-bandgap perovskite solar cells used in tandems.[19] In our model, the reverse saturation current for the perovskite solar cells and silicon solar cells was determined using the detailed balance limit for a minimum reverse saturation current. However, the model is unaffected by perturbations in the value of the reverse saturation current because, the currents running through the devices in the model are always many orders of magnitude larger than the reverse saturation current and therefore leave the model unaffected. Perovskite solar cells with slightly narrower bandgaps can generate a higher current, but that does not substantially change the conclusions in this manuscript. The breakdown voltage has been observed to vary between −1 and −4 V for reasons that are not yet fully understood. At the end of this manuscript, we will discuss the implications of changing the breakdown voltage. When operating near the global MPP, marked by the red vertical line in Figure 1, the partially shaded cell is forced into reverse bias. The current through the module is equal to the current running through each cell; therefore, overlaying the current through the module on the cell *I–V* curve gives the operating point of both the unshaded and partially shaded devices (**Figure 2**).

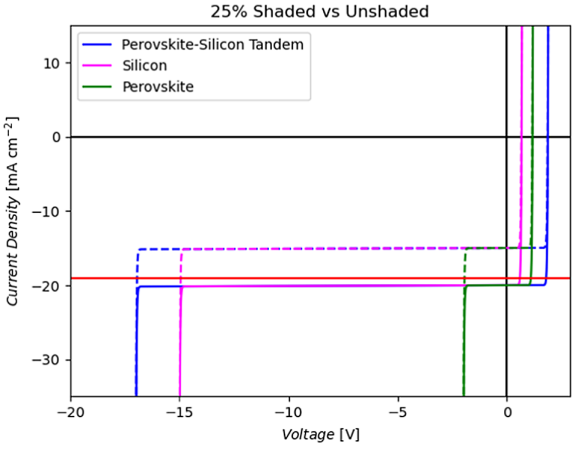

Figure 2. Plotted are simulated *I–V* curves for silicon single junction (pink), perovskite single junction (green), and a silicon–perovskite tandem (blue). The silicon IV curve shown is modeled after a silicon sub-cell in a current matched perovskite silicon two terminal tandem, hence the reduced short circuit current density of 20 mA cm^{-2}. There are plots for both 25% shaded cells (dashed) and fully illuminated cells (solid). Red horizontal line: this corresponds to the maximum power current of an unshaded module.

3. Bypass Diodes

The maximum reverse bias ($V_{\text{rev, max}}$) that can be applied to a single solar cell in a module of N cells by a typical power point tracker is $V_{\text{rev, max}} = V_{\text{oc}} \times (N-1)$. This occurs in the case that one cell in the module is completely shaded, and the others are all completely unshaded. If the magnitude of this voltage is insufficient to cause current to pass in the shaded cell, then the module will be current limited by the shaded cell. Therefore, a strategy for protecting cells is to reduce the solar cell string length to prevent the shaded cell from going into reverse bias breakdown. However, reducing the number of cells in a module is undesirable, because using larger cells would increase the current, which would lead to more resistive losses. One method to decrease $V_{\text{rev,max}}$ without sacrificing module voltage is to place Schottky diodes, also known as bypass diodes, in an anti-parallel configuration with the cells in the module. When the module is unshaded, ideally, the bypass diodes pass no current, thus dissipating no power and leaving the module unaffected. When a cell is shaded, however, the reverse bias turns the bypass diode on before the shaded cell passes current. This protects the shaded cell and allows the module to continue outputting the global MPP current, but at a reduced voltage.

Unfortunately, there are several downsides to use bypass diodes. When a bypass diode is on, none of the cells in parallel with the bypass diode are producing power. This effect can be mitigated by increasing the number of bypass diodes and reducing the number of cells in parallel with a single diode, which reduces the number of cells that stop producing power. However, this adds complexity and, therefore, cost (about \$0.10/diode).[20]

Traditionally, for monolithically integrated modules, an additional challenge is presented when implementing bypass diodes. If current is not passing through the shaded cell, then the current must travel around the shaded cell, to the edge of the module, to reach the bypass diode, then from the edge to the center. This extra path length causes additional resistive loss and associated Joule heating. In this situation, the electrode material becomes very important. The current will typically need to traverse a length of at least 0.5 m, which is problematic for carbon or transparent conducting oxide (TCO)-based electrodes, as they do not have sufficient conductivity to prevent large voltage drops. To avoid these resistive losses, 1 μm-thick metal electrodes would be needed in addition to the carbon or TCO-based electrode to prevent the associated voltage loss of more than 250 mV.[1] Another possible configuration that circumvents this issue is a shingled architecture with a metal layer connecting the shingles. As before, and in this configuration, the bypass diodes are at the edge of the module.[3] Many metals react with metal halide perovskites under typical operational conditions;[21–35] therefore, additional layers and care would be needed to ensure the success of this method.

Another issue associated with bypass diodes is the Joule heating that occurs at the diode when the diode is on. The amount of Joule heating in a bypass diode is proportional to the current passed through the diode and the turn-on voltage of the bypass diode.[36] When it is on, a bypass diode dissipates heat in the same way that a solar cell undergoing breakdown would. This heating can be reduced through the use of low threshold bypass diodes that turn on at smaller voltages, reducing the Joule heating. Low threshold diodes are not in common use in commercial panels, as they are currently about 10× more expensive than more traditional commercial Schottky diodes used in this application.[20] It is of critical importance to understand that if there are not enough bypass diodes, the maximum reverse bias voltage will be larger than the cell breakdown voltage, and therefore, the bypass diodes will never turn on and will not prevent reverse bias damage or degradation in the shaded cell.

4. Maximum Allowable $V_{\text{rev, max}}$ to Prevent Reverse Bias Breakdown

The maximum number of solar cells per bypass diode that can be used while still having the diodes turn on is

$$N_{\text{string,max}} = \left\lfloor \frac{V_{\text{br}} - V_{\text{to}}}{V_{\text{oc}}} + 1 \right\rfloor \tag{1}$$

where V_{br} is the reverse bias breakdown voltage, and V_{to} is the bypass diode turn-on voltage. V_{to} is typically 0.6 V for a normal Schottky diode.

This equation can be understood with a quick thought experiment. Suppose we have a module with M bypass diodes and $M \times N$ cells, where N is the number of cells per bypass diode. Let one of the cells become completely shaded (**Figure 3**). This will turn on one of the M bypass diodes. All the current will pass through this diode instead of the string the diode protects. Two things are now known. The voltage across the cells in parallel with the bypass diode is the same as the voltage across the bypass diode, and, in this simple case, all the current in the module is redirected through the diode, not the group of N cells (1 shaded cell and $N-1$ unshaded cells). This means that the $N-1$ unshaded cells in parallel with the activated diode are at V_{oc}. The rest of the cells in the module are unaffected and are still running at MPP. From Kirchhoff's voltage law, we know that the voltage across the shaded cell must equal the sum of the voltages of the bypass diode and unshaded cells. Therefore, for a bypass diode turn-on voltage V_{to}, the voltage on the shaded cell

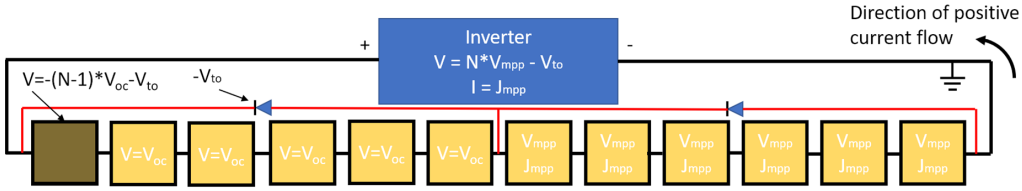

Figure 3. A simple diagram showing the shading of a single cell in a module. Using the convention defined earlier, $N = 6$ and $M = 2$.

is $V_{shaded} = -(N-1) \times V_{oc} - V_{to}$. If there is one bypass diode per cell ($N = 1$), the voltage on the shaded cell is simply the turn-on voltage of the bypass diode. For every unshaded cell in parallel with the diode, the reverse voltage on the shaded cell increases by V_{oc} of the unshaded cells. This brings up the issue that if the number of cells per bypass diode (N) is too large, the shaded cell will breakdown before the bypass diode turns on. Using silicon cells as an example, if we have $N = 11$, a bypass diode turn-on voltage of 0.6 V, and a V_{oc} of 0.7 V, a shaded cell will have a reverse voltage of −7.6 V.

5. Module and Cell Orientation Design

The maximum reverse bias voltage a fully shaded cell could experience can be reduced by changing the module topology from a series-connected module (**Figure 4**) to a series–parallel module (**Figure 5**). In a series–parallel module, cells are wired into rows of the desired length; then, those rows are connected in parallel. If a single cell were to be partially shaded in a module with a series-parallel topology (Figure 5), then like the fully series connected module, the power voltage curve would have two peaks. The higher voltage peak corresponds to the situation in which the shaded cell is operating at the maximum power point and the normally illuminated cells in that particular string are operating at voltages slightly higher than their maximum power point, but with a reduced current matching the partially shaded cell. The lower voltage peak corresponds to the situation in which the normally illuminated cells in the string with the shaded cell are operating at their maximum power point, and the shaded cell is placed into reverse bias in order to pass the current produced by the other cells. It is critical to note that the normally illuminated cells in the other unaffected strings are now operating at reduced voltages and therefore no longer at maximum power point. The number of cells in series, the number of strings in parallel, and the amount of shading will dictate which of the two peaks is the global maximum. In order to prevent the lower voltage curve from ever being the global maximum power point,

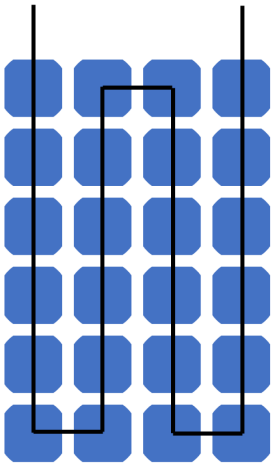

Figure 4. A standard series-connected wafer style panel topology. In this orientation, it is easy to place bypass diodes on the top and bottom of the panel. If the modules were rotated 90°, the easiest location for the bypass diodes would be on the left and right edges.

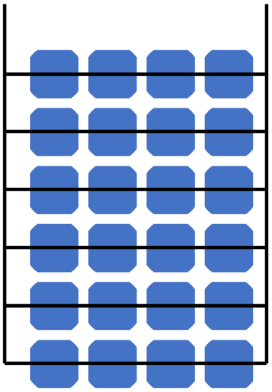

Figure 5. A series–parallel-connected wafer style panel topology. In this topology, the number of cells in series can be reduced without the use of bypass diodes. Connecting the cells across the shorter side reduces the number of series-connected cells further when compared with cells connected across the longer side. Orienting the cell wiring to run horizontally ensures that any accumulated material across the bottom of the device reduces the current for all cells in one row, rather than one cell in each column.

the number of cells in the string can be reduced to push the lower voltage peak into the third quadrant. Stated another way, reducing the number of cells in the string can be reduced to ensure $V_{rev,\,max}$ has a smaller magnitude than the breakdown voltage of the individual cell. The main downside of this configuration is that the panel has an overall smaller voltage and a larger current compared with the series-connected module. This reduces module efficiency, because larger currents exacerbate resistive losses associated with extracting current from the module to the junction box. It should be noted that the resistive losses at the cell level and the string level are the same in both topologies. The extra losses occur after the strings are connected together, because that is where the current is larger than a series topology.

6. Single-Junction Perovskite Cells versus Tandems

Kirchhoff's laws state that voltages add for circuit elements in series. This means that the open circuit voltage of a tandem is determined by adding the open circuit voltages of the cells in that tandem. Similarly, the breakdown voltage of a tandem is determined by adding the breakdown voltages of its constituent subcells. For example, consider the dark current–voltage curves for aperovskite cell and a silicon cell. If both cells pass J_{mpp}, then both are in reverse bias, at their respective breakdown voltages. Placing the two cells in series means that the voltage drop across both is simply the sum of the two breakdown voltages (Figure 2). When in the breakdown regime, because the two subcells are connected in series, Kirchhoff's law demands the currents must be equal. There are no assumptions regarding the distribution of voltage across the sub-cells. The distribution of voltages across the sub-cells is unique and dictated by solutions to Kirchhoff's voltage and current laws. In the case of a shaded tandem operating at reverse breakdown, the current passing

Table 1. A comparison of the maximum string length to prevent reverse bias breakdown across different solar cell technologies. The breakdown voltage of perovskite cells can vary, so these values are just examples.

Type of module	V_{oc} [V]	V_{br} [V]	$N_{string,\ max}$
Silicon	≈0.7 V	≈15 V	≈21
Perovskite–silicon tandem	≈1.9 V = 1.2 V + 0.7 V	≈17 V = 2 V + 15 V	≈9
Perovskite	≈1.2 V	≈2 V	≈2
Perovskite–perovskite tandem	≈2 V = 1.2 V + 0.8 V	≈4 V = 2 V + 2 V	≈2

through the tandem cell is the module current (about 20 mA cm^{-2} in this model). Therefore, the current through each sub-cell is also 20 mA cm^{-2}. There is only one voltage that corresponds to this current, therefore the silicon cell must operate at −15 V and the perovskite cell must operate at −2 V. As a silicon cell has a larger breakdown voltage and a smaller V_{oc} than a perovskite cell, using the equation mentioned earlier, it can be determined that a perovskite-Si tandem cell can support more cells per bypass diode than a single-junction perovskite cell. More simply, $N_{string,\ max}$ is larger for perovskite-Si tandems than for perovskite single-junction cells. See **Table 1** for a comparison of different values of $N_{string,\ max}$ for different photovoltaic technologies. In addition to substantially increasing the breakdown voltage and the number of cells that can be protected by one bypass diode, another advantage of making panels with perovskite–silicon tandems (instead of monolithically integrated thin-film panels) is that it is relatively straightforward to run a metal ribbon to the bypass diodes that are typically housed in the junction box.

7. Various Cell Geometries and Orientations in Modules

One strategy for mitigating some of the reverse bias shading problems is to make a monolithically integrated module with cells that are as long as the module. Panels from First Solar, which contain thin-film CdTe cells, are over 1 m tall and have vertically oriented cells connected in series across the panel.[37] In this case, a shading event across an entire cell is difficult, but not impossible, to encounter. The First Solar does not cover damage due to partial shading in its warranty.[37] For a utility-scale application, running the cells vertically (**Figure 6**b) protects a panel from the daily shading event of the panel in the adjacent row, which casts a shadow horizontally along the bottom of the entire panel.

For debris such as accumulated dirt, snow, or other opaque material that can flow, most geometries will be affected similarly, as, initially, the debris will likely uniformly cover the whole panel. If, however, the material slides to the bottom of the panel and accumulates there, the vertical-cell geometry is much more robust, as each vertical line will be approximately equally covered by the accumulated material (Figure 6b). This is not a perfect solution, as there are also situations in which the material does not move down as a whole and can create shading patterns that run vertically.

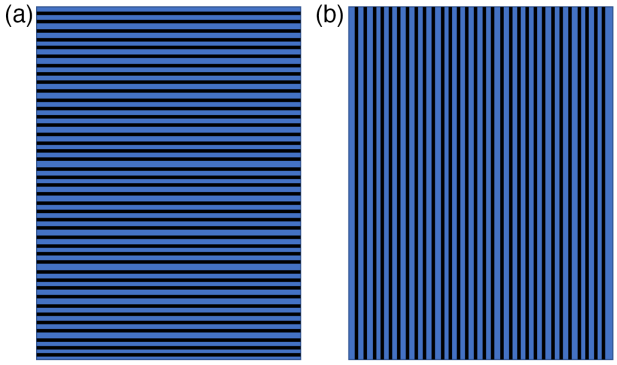

Figure 6. Two orientations for a monolithically interconnected module. a) The left orientation is a tall aspect ratio module with horizontally oriented interconnections. b) The right orientation is a tall aspect ratio module with vertically oriented interconnections.

Silicon panels made of wafers can easily be shaded from the same situations as previously mentioned. Individual silicon cells in a panel are also more prone to being completely covered by nearby objects. These objects could be fallen leaves from trees or bird droppings. In a residential application, it is not hard to imagine additional small objects, such as a frisbee,[38] covering one cell in a conventional (i.e., nonshingled) module.

For the silicon wafer style series–parallel panel with 6" × 6" cells, connecting the cells horizontally (Figure 5) could mitigate the impact of accumulated material at the bottom of the panel. The opaque material would reduce the current of all cells in one row. This would keep the currents across all cells in a row well matched, preventing reverse bias of any of the cells in the bottom row. If the aspect ratio of these panels is tall, rather than wide, then the number of cells per row will be reduced, effectively reducing $V_{rev,\ max}$.

8. Hot Spots in Silicon Modules with Bypass Diodes

Silicon solar cells have a pre-breakdown voltage region where some current begins to pass through the solar cell before the full breakdown occurs.[39,40] Silicon solar cells typically have three different mechanisms of reverse bias breakdown, commonly referred to as type I, type II, and type III.[41] Type-I breakdown typically occurs between −4 and −9 V and is mainly caused by aluminum contamination of the surface. Type-II breakdown typically occurs between −9 and −13 V and is mainly caused by defects.[42] Finally, Type-III breakdown typically occurs beyond −13 V, where avalanche breakdown is induced at etch pits. Therefore, a silicon solar cell without contaminants will break down beyond −13 V. In all three types of breakdown, the current is not passed uniformly. This leads to local hot spots, which can increase degradation rates in reverse bias. Interdigitated back contact silicon solar cells add a fourth reverse breakdown mechanism through some clever engineering of the cell architecture. In interdigitated back contact solar cells (IBC) cells, the p^+ and n^+ regions are fabricated to be in contact with each other, to form a Zener diode, which heavily reduces the breakdown voltage of the cell and acts as a built-in bypass diode. IBC cells pass reverse

current uniformly through the cell, which does not produce local hotspots.[43]

Silicon modules commonly use 20 cells per bypass diode and are designed to prevent silicon cells with the breakdown voltages exceeding 15 V from experiencing full breakdown, whereas minimizing the number of bypass diodes used to keep complexity and cost low. It should be kept in mind that as defects assist reverse bias breakdown, some silicon solar cells can have a smaller breakdown voltage than others.[40,42,44] If a silicon cell with small reverse bias breakdown is shaded, then it is easy to imagine the bypass diode not turning on, forcing the silicon cell to pass all the current of the module, causing significant Joule heating.[40] In the event that a bypass diode does turn on, the pre-breakdown region can cause shaded silicon cells to pass some of the module current, whereas the bypass diode passes the rest of the current. This will cause moderate heating both at the shaded silicon cell and the bypass diode.

If a shading event was to occur with a perovskite–silicon module and there were not enough bypass diodes, then the Joule heating through the silicon cell would likely be so large that the temperatures reached would rapidly degrade theperovskite top layer. Studies on silicon single-junction cells show that the temperatures can easily exceed 100 °C, which is hot enough to substantially increase the degradation rate of a perovskite cell.[39] This means that the number of perovskite–silicon cells put in parallel with a bypass diode must not be so large that a lower quality silicon bottom cell causes a bypass diode to not turn on in a partial shading event.

9. Conclusion

Finding solutions to the problems introduced by partial shading of perovskite solar modules is paramount to the success of perovskite solar as a transformative technology and should be considered when making decisions on whether to deploy single-junction perovskites, perovskite–silicon tandems, perovskite-copper indium gallium selenide (CIGS) tandems, or all-perovskite tandems as well as whether to connect singulated cells with wires/ribbons or to use a monolithically integrated approach. A substantial advantage of perovskite–silicon tandems is that the silicon significantly raises the breakdown voltage and increases the number of cells that can be protected by one bypass diode. It is considerably easier to run metal ribbon from singulated cells to bypass diodes, which is why bypass diodes are deployed in silicon panels, but almost never used in thin-film panels.[3]

If monolithically integrated thin panels are selected, the panels should be tall and have vertically oriented cells. If a decision is made that it is impractical to use bypass diodes, then the panels should probably be deployed in utility-scale power generating plants where they can be protected from partial shading conditions by ensuring that things such as nearby trees, buildings, and poles or well-intentioned cleaning procedures do not cause problems.

Far and away, the most ideal solution is for a perovskite solar cell to have a low reverse bias breakdown voltage and not degrade while in the breakdown regime. This would allow the perovskite solar cell to act as its own bypass diode, solving the problem for any partial shading geometry. In addition, a small breakdown voltage minimizes both the amount of power the panel must dissipate to pass current through the shaded device, which reduces the power output of the unshaded cells, and the local heating experienced by the shaded cell, preventing hotspots. There are multiple pathways to address this challenge, and the ultimate embodiment may depend on the specifics of the application and the aspects of the manufacturing process.

Acknowledgements

This material was based on work supported by the U.S. Department of Energy's Office of Energy Efficiency and Renewable Energy (EERE) under Solar Energy Technologies Office (SETO) Agreement Number DE-EE0008551.

Conflict of Interest

The authors declare no conflict of interest.

Keywords

degradation, module designs, perovskites, reverse bias, simulation

Received: March 31, 2021
Revised: April 23, 2021
Published online:

[1] A. R. Bowring, L. Bertoluzzi, B. C. O'Regan, M. D. McGehee, *Adv. Energy Mater.* **2018**, *8*, 1.
[2] Best Research-Cell Efficiency Chart, https://www.nrel.gov/pv/assets/pdfs/best-research-cell-efficiencies.20200925.pdf (accessed: September 2020).
[3] J. Werner, C. C. Boyd, T. Moot, E. J. Wolf, R. M. France, S. A. Johnson, M. F. A. M. Van Hest, J. M. Luther, K. Zhu, J. J. Berry, M. D. McGehee, *Energy Environ. Sci.* **2020**, *13*, 3393.
[4] S. P. Dunfield, L. Bliss, F. Zhang, J. M. Luther, K. Zhu, M. F. A. M. van Hest, M. O. Reese, J. J. Berry, *Adv. Energy Mater.* **2020**, *10*, 1.
[5] M. Stolterfoht, M. Grischek, P. Caprioglio, C. M. Wolff, E. Gutierrez-Partida, F. Peña-Camargo, D. Rothhardt, S. Zhang, M. Raoufi, J. Wolansky, M. Abdi-Jalebi, S. D. Stranks, S. Albrecht, T. Kirchartz, D. Neher, *Adv. Mater.* **2020**, *32*, 2000080.
[6] M. T. Hörantner, T. Leijtens, M. E. Ziffer, G. E. Eperon, M. G. Christoforo, M. D. McGehee, H. J. Snaith, *ACS Energy Lett.* **2017**, *2*, 2506.
[7] R. Lin, K. Xiao, Z. Qin, Q. Han, C. Zhang, M. Wei, M. I. Saidaminov, Y. Gao, J. Xu, M. Xiao, A. Li, J. Zhu, E. H. Sargent, H. Tan, *Nat. Energy* **2019**, *4*, 864.
[8] L. Bertoluzzi, J. B. Patel, K. A. Bush, C. C. Boyd, R. A. Kerner, B. C. O'Regan, M. D. McGehee, *Adv. Energy Mater.* **2021**, *11*, 2002614.
[9] C. G. Bischak, A. B. Wong, E. Lin, D. T. Limmer, P. Yang, N. S. Ginsberg, *J. Phys. Chem. Lett.* **2018**, *9*, 3998.
[10] R. A. Z. Razera, D. A. Jacobs, F. Fu, P. Fiala, M. Dussouillez, F. Sahli, T. C. J. Yang, L. Ding, A. Walter, A. F. Feil, H. I. Boudinov, S. Nicolay, C. Ballif, Q. Jeangros, *J. Mater. Chem. A* **2020**, *8*, 242.
[11] J. Qian, M. Ernst, D. Walter, M. A. Mahmud, P. Hacke, K. Weber, M. Al-Jassim, A. Blakers, *Sustain. Energy Fuels* **2020**, *4*, 4067.
[12] L. Bertoluzzi, C. C. Boyd, N. Rolston, J. Xu, R. Prasanna, B. C. O'Regan, M. D. McGehee, *Joule* **2020**, *4*, 109.
[13] J. Qian, A. F. Thomson, Y. Wu, K. J. Weber, A. W. Blakers, *ACS Appl. Energy Mater.* **2018**, *1*, 3025.

[14] S. Guo, T. M. Walsh, A. G. Aberle, M. Peters, in *2012 38th IEEE Photovoltaic Specialists Conf.*, IEEE, Piscataway, NJ **2012**.
[15] S. Vemuru, P. Singh, M. Niamat, in *2012 IEEE Int. Conf. Electro/Information Technology*, IEEE, Piscataway, NJ **2012**.
[16] A. Kajihara, T. Harakawa, in *Proc. IEEE Int. Conf. Industrial. Technolofy*, IEEE, Piscataway, NJ **2005**.
[17] M. Q. Duong, G. N. Sava, G. Ionescu, H. Necula, S. Leva, M. Mussetta, in *Conf. Proc.–2017 17th IEEE Int. Conf. Environment and Electrical Engineering 2017 1st IEEE Industrial Commercial Power Systems Europe EEEIC/I CPS Eur. 2017*, IEEE, Piscataway, NJ **2017**.
[18] V. Quaschning, R. Hanitsch, *Sol. Energy* **1996**, *56*, 513.
[19] J. Xu, C. C. Boyd, Z. J. Yu, A. F. Palmstrom, D. J. Witter, B. W. Larson, R. M. France, J. Werner, S. P. Harvey, E. J. Wolf, W. Weigand, S. Manzoor, M. F. A. M. Van Hest, J. J. Berry, J. M. Luther, Z. C. Holman, M. D. McGehee, *Science.* **2020**, *367*, 1097.
[20] B. B. Pannebakker, A. C. de Waal, W. G. J. H. M. van Sark, *Prog. Photovoltaics Res. Appl.* **2017**, *25*, 836.
[21] C. C. Boyd, R. Cheacharoen, K. A. Bush, R. Prasanna, T. Leijtens, M. D. McGehee, *ACS Energy Lett.* **2018**, *3*, 1772.
[22] T. Leijtens, K. Bush, R. Cheacharoen, R. Beal, A. Bowring, M. D. McGehee, *J. Mater. Chem. A* **2017**, *5*, 11483.
[23] N. N. Shlenskaya, N. A. Belich, M. Grätzel, E. A. Goodilin, A. B. Tarasov, *J. Mater. Chem. A* **2018**, *6*, 1780.
[24] G. Y. Kim, A. Senocrate, T. Y. Yang, G. Gregori, M. Grätzel, J. Maier, *Nat. Mater.* **2018**, *17*, 445.
[25] K. Domanski, J. P. Correa-Baena, N. Mine, M. K. Nazeeruddin, A. Abate, M. Saliba, W. Tress, A. Hagfeldt, M. Grätzel, *ACS Nano* **2016**, *10*, 6306.
[26] R. A. Kerner, L. Zhao, S. P. Harvey, J. J. Berry, J. Schwartz, B. P. Rand, *ACS Energy Lett.* **2020**, 3352.
[27] L. Zhao, R. A. Kerner, Z. Xiao, Y. L. Lin, K. M. Lee, J. Schwartz, B. P. Rand, *ACS Energy Lett.* **2016**, *1*, 595.
[28] N. Aristidou, C. Eames, I. Sanchez-Molina, X. Bu, J. Kosco, M. Saiful Islam, S. A. Haque, *Nat. Commun.* **2017**, *8*, 1.
[29] B. Conings, J. Drijkoningen, N. Gauquelin, A. Babayigit, J. D'Haen, L. D'Olieslaeger, A. Ethirajan, J. Verbeeck, J. Manca, E. Mosconi, F. De Angelis, H. G. Boyen, *Adv. Energy Mater.* **2015**, *5*, 1.
[30] T. Leijtens, G. E. Eperon, S. Pathak, A. Abate, M. M. Lee, H. J. Snaith, *Nat. Commun.* **2013**, *4*, 1.
[31] Y. Han, S. Meyer, Y. Dkhissi, K. Weber, J. M. Pringle, U. Bach, L. Spiccia, Y. B. Cheng, *J. Mater. Chem. A* **2015**, *3*, 8139.
[32] Y. Kato, L. K. Ono, M. V. Lee, S. Wang, S. R. Raga, Y. Qi, *Adv. Mater. Interfaces* **2015**, *2*, 2.
[33] J. Li, Q. Dong, N. Li, L. Wang, *Adv. Energy Mater.* **2017**, *7*, 1.
[34] C. Besleaga, L. E. Abramiuc, V. Stancu, A. G. Tomulescu, M. Sima, L. Trinca, N. Plugaru, L. Pintilie, G. A. Nemnes, M. Iliescu, H. G. Svavarsson, A. Manolescu, I. Pintilie, *J. Phys. Chem. Lett.* **2016**, *7*, 5168.
[35] H. Lee, C. Lee, *Adv. Energy Mater.* **2018**, *8*, 1.
[36] B. G. Streetman, S. Banerjee, *Prentice Hall Ser. Solid State Phys. Electron*, 6th ed. **2000**, p. 197
[37] First Solar, First Solar Series 6TM Module | USER GUIDE PD-5-200-06, http://www.firstsolar.com/-/media/First-Solar/Technical-Documents/User-Guides/Series-6-User-Guide.ashx?la=en (accessed: September 2020).
[38] E. E. Headrick, US3359678A, **1965**.
[39] M. C. S. Ino Geisemeyer, F. Fertig, W. Warta, S. Rein, in *27th European Photovoltaic Solar Energy Conf. and Exhibition*, IEEE, Piscataway, NJ **2014**.
[40] K. A. Kim, P. T. Krein, in *2013 IEEE Energy Conversion Congress and Exposition ECCE 2013*, IEEE, Piscataway, NJ **2013**, p. 1007.
[41] O. Breitenstein, J. Bauer, K. Bothe, W. Kwapil, D. Lausch, U. Rau, J. Schmidt, M. Schneemann, M. C. Schubert, J. M. Wagner, W. Warta, *J. Appl. Phys.* **2011**, *109*, 071101.
[42] P. Tománek, P. Škarvada, R. MacKů, L. Grmela, *Adv. Opt. Technol.* **2010**, *2010*, 805325.
[43] R. Müller, C. Reichel, J. Schrof, M. Padilla, M. Selinger, I. Geisemeyer, J. Benick, M. Hermle, *Sol. Energy Mater. Sol. Cells* **2015**, *142*, 54.
[44] P. Škarvada, Tománek, L. Grmela, S. J. Smith, *Sol. Energy Mater. Sol. Cells* **2010**, *94*, 2358.

Eli Wolf obtained his B.S. degree in physics from the College of Creative Studies at the University of California, Santa Barbara, in 2015. He completed his master's degree in applied physics in 2018 and is currently pursuing his Ph.D. degree in applied physics at Stanford University under the supervision of Prof. Michael D. McGehee. His work focuses on quantifying various degradation mechanisms in lead halide perovskite solar cells, particularly degradation caused by reverse bias and residual film stress.

Isaac Gould obtained his bachelor's degree in physics and chemistry from the Honors College at The College of Charleston, SC, in 2016. He is currently a Ph.D. candidate in the Material Science and Engineering program at the University of Colorado Boulder, investigating reverse bias stability of lead halide perovskite solar cells.

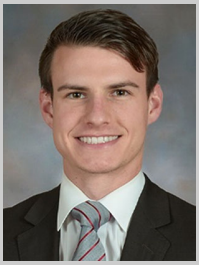

Lyle Bliss obtained his bachelor's degree in chemical engineering from the School for Engineering of Matter, Transport, and Energy at Arizona State University, in 2017. He is currently working toward his Ph.D. degree with the CHBE Department at the University of Colorado Boulder. His primary research area is scalable perovskite photovoltaics, specifically exploring degradation caused by laser processing of perovskite solar modules at the National Renewable Energy Laboratory in Golden, CO.

Joseph Berry is a principal scientist at the National Renewable Energy Laboratory (NREL) working on halide perovskite solar cells. His efforts at NREL emphasize relating basic interfacial properties to relevant device level behaviors in traditional and novel semiconductor heterostructures, including oxides, organics, and most recently hybrid semiconductors. He is also a principal investigator on the NREL Lead Department of Energy, Solar Energy Technology Offices "De-risking Halide Perovskite Solar Cells" program, the director of the US-Manufacturing of Advanced Perovskites (US-MAP) Consortium, and a fellow at RASEI, a joint energy institute between the University of Colorado Boulder and NREL.

Mike McGehee is a professor with the Chemical and Biological Engineering Department at the University of Colorado Boulder. He is the associate director of the Materials Science and Engineering Program and has a joint appointment at the National Renewable Energy Laboratory. He was a professor with the Materials Science and Engineering Department at Stanford University for 18 years and a senior fellow of the Precourt Institute for Energy. His current research interests are developing new materials for smart windows and solar cells. He received his Ph.D. degree in materials science from the University of California, Santa Barbara.